DOI: 10.1002/anie.200((will be filled in by the edit

Cryo-Electron Tomography reveals Confined Complex Morphologies from Tripeptide-containing Amphiphilic Double Comb Diblock Copolymers

Alison L. Parry, Paul H.H. Bomans, Simon J. Holder, Nico A.J.M. Sommerdijk* and Stefano C.G. Biagini**

((Dedication----optional))

The property of amphiphilic block copolymers to form self-assembled structures in aqueous media has been known and studied for many years.[1] This form of self-assembly is known to produce a wide range of morphologies, the most common ones being spherical micelles, cylindrical micelles and vesicles.[1] Over the past decade a number of other morphologies have been observed including stacked micelles,[2] toroids,[3] hexagonally packed hoola hoops,[4] helices[5] and branched structures.[6] Initially linear diblock copolymers were the main type of macromolecules used for these studies, however, in later investigations the toolbox of polymer self-assembly was extended to the use of dendrimers,[7] and branched[8] polymer segments as one of the blocks, but also ABA,[9] ABC,[10] and multi[11] block copolymers have been explored.

Furthermore, the desire to direct the polymer assembly process through molecular design resulted in various bio-inspired approaches. It was demonstrated that in addition to synthetic monomers also building blocks from biological origin could be used, exploring the use of peptide-derived monomers,[5] poly(amino acids),[12] specific peptide sequences[13] and even complete proteins[14] and enzymes[15] to construct (one of) the polymer blocks.

A separate class of amphiphiles is formed by comb-like block polymers. These have one or more segments composed of a central polymer backbone with polymeric or oligomeric side chains. Comb-like polymers exist with hydrophobic[16] as well as hydrophilic side chains[17] and also as random copolymers with both types of side chains[18]. Comb-like polymers have been coupled to other linear[19] or dendritic[20] segments forming AB[19,20] as well as ABA[21] type bloc copolymers. Gnanou et al described a ROMP strategy towards amphiphilic block copolymers using norbornene-based macromonomers with polystyrene and poly(ethylene oxide) side chains, respectively.[22] Recently some of us used the same strategy towards the synthesis of norbornene-based double comb diblock polymers containing oligo(ethylene oxide) (OEG) side chains in one block and a specific peptide sequence in the other block.[23.]

Here we report how this new polymer architecture (see also SI2) allows us to specifically modify the self-assembly behaviour through the introduction of different amino acids in the hydrophobic block. Moreover, we show how the complex morphologies resulting from the aggregation of these amphiphilic double comb diblock copolymers can be analysed and visualized with nanometer detail using cryo electron tomography (cryoET).

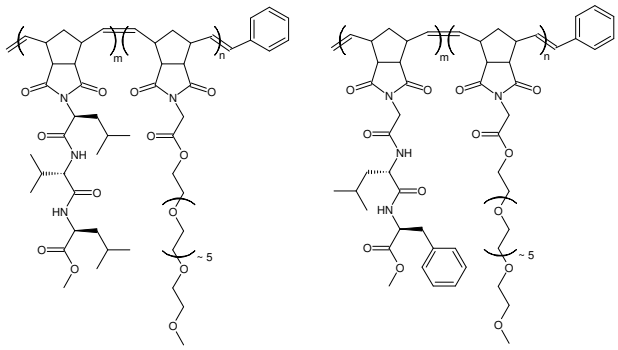

1 **PNOEG-PNGLF** m=50, n=50
2 **PNOEG-PNLVL** m=50, n=50
3 **PNOEG** m=0, n=50
4 **PNGLF** m=50, n=0
5 **PNLVL** m=50, n=0
6 **PNOEG-PNGGG** m=50, n=50
7 **PNOEG-PNGL** m=0, n=50

The block copolymers (10 mg) were dispersed in water by dissolution in a small volume of DMSO (3 cm^3) followed by the drop wise addition of water (7 cm^3) under vigorous stirring.[24]. Samples were subsequently dialysed against distilled water for 48 hours to obtain a final concentration of copolymer in water of 1 g dm^{-3} DLS indicated the formation of stable aggregates with diameters of 50-450nm for **PNOEG-PNGLF (1)** and 80-280 nm for **PNOEG-PNLVL (2)** (see Fig SI1). The morphology of these aggregates was investigated with conventional (negative staining) as well as cryogenic (cryo) TEM which both showed that the two block copolymers both formed unprecedented, complex morphologies (figure 1 and 2). GLF-based block copolymer **1** was observed to form large spherical aggregates which showed internal microphase separation (Fig. 1a,b). The LVL-derived block copolymer (**2**) also displayed an unusual aggregate morphology, which appeared to consist of tightly coiled worm-like micelles (fig 2a,b).

CryoTEM has now been established as an important technique for the 2D visualization of a large range of self-assembled structures in solution.[25] CryoET involves the acquisition of a series of

[*] Dr. Alison L. Parry, Dr. Simon J. Holder, Dr. Stefano C.G. Biagini
Functional Materials Group, Chemical Laboratory, School of Physical Sciences,
University of Kent at Canterbury
Canterbury, Kent, CT2 7NR. UK
Fax: (+) 44 1227 827558
E-mail: S.C.G.Biagini@kent.ac.uk , S.J.Holder@kent.ac.uk

Paul H.H. Bomans, Dr. Nico A.J.M. Sommerdijk
Laboratory of Materials and Interface Chemistry and Soft Matter Cryo-TEM Research Unit,
Eindhoven University of Technology,
PO Box 513, 5600 MB, Eindhoven, The Netherlands.
Email: N.Sommerdijk@tue.nl

The authors thank Dr. K. Lyakhova for valuable discussions.

Supporting information for this article is available on the WWW under http://www.angewandte.org or from the author.

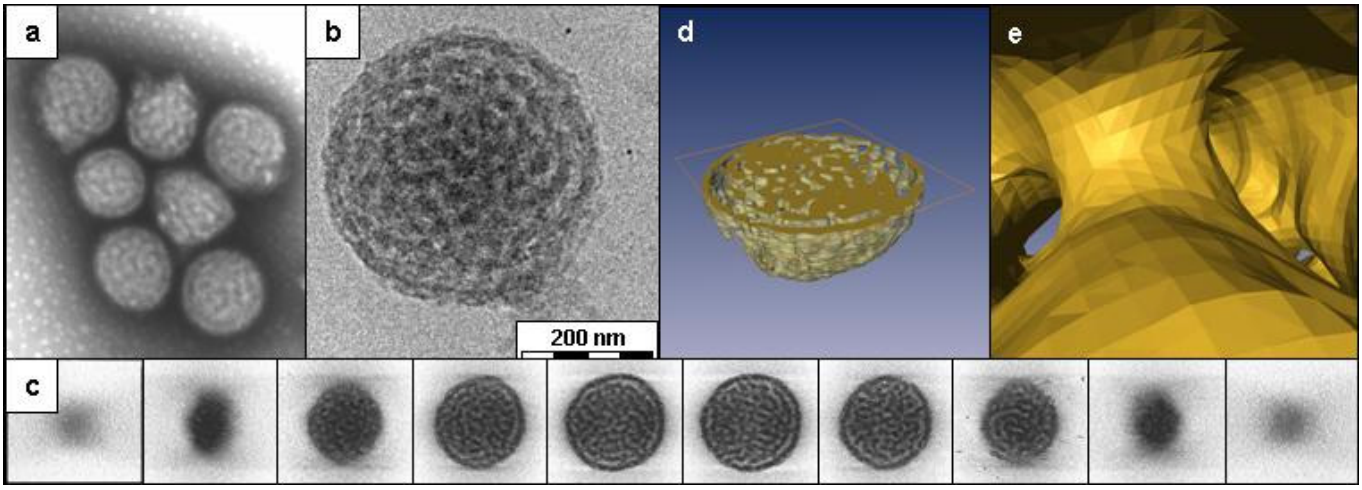

Figure 1. TEM analysis of aggregates of **PNOEG-PNGLF** (**1**). a) Conventional TEM using negative staining, b) cryoTEM image of a vitrified film, c) gallery of z slices showing different cross sections of a 3D SIRT reconstruction of a tomographic series recorded from the vitrified film in b) d-e) Visualization of the segmented volume showing d) a cross section of the aggregate and e) a view from within the hydrated channels.

cryoTEM images under different tilt angles and the subsequent computer-assisted reconstruction of the original 3D volume. Although cryoET has been recognized as a strong and emerging technique in the biological sciences,[26] it is still virtually unexplored for the analysis of samples from synthetic origin.[27]

To completely elucidate the structure of the aggregates of **1** and **2,** vitrified samples were studied using low–dose cryoET. Tilt series were recorded under low dose conditions (total dose 100 e^{-}·Å^{-2}) by collecting images between -70° and + 70° with 1° tilt increments and the 3D volume was reconstructed using the SIRT algorithm (Figures 1 and 2).

Analysis of the reconstructed 3D volume shows that the aggregates of **1** consist of a spherical aggregate of which the interior is formed by an interpenetrating network of dark, electron opaque, and lighter, almost electron transparent regions forming a bicontinuous assembly in which the branched network of worm-like hydrophobic peptide-containing segments are segregated from channels containing the hydrated OEG moieties. Detailed analysis of the individual slices (Fig 1c) from the reconstructed volume revealed that the hydrophobic domains had an average cross section of 20 ± 2 nm whereas the average cross section of the water channels was 15± 2 nm.[28] The z-slices of the reconstruction further showed that the apparent shell which encloses the bicontinous network inside the aggregates has perforations that connect the internal and external aqueous phases. Segmentation was used to generate graphical representations that clearly demonstrate the 3D structure of these aggregates, highlighting both the bicontinuous structure and the perforations in the encapsulating shell (fig. 1d-e).

Inspection of the reconstructed volume of the aggregates of **2** revealed that the coiled globular aggregates consist of single worm-like micelles with diameters of 20 ± 2 nm. Moreover, the aggregate is folded such that linear micellar segments are placed at the same average distance of ~ 20-25 nm with respect to each within the aggregate. Again segmentation was used to illustrate the morphological features that are not evident from the x-y cross sections of the 3D volume (Fig 2c) The resulting 3D visualization of the volume of the aggregate (Fig 2d) was further reduced by thinning (inset) and skeletonization (Fig 2e) to show that these worm-like structures contained several branches and loops within a single aggregate.

To investigate the role of the different macromolecular components in the self-assembly of the block copolymers we also investigated with conventional TEM the aggregation behaviour of the different polymer blocks (**3**-**5**) alone as well as that of block copolymers **6** and **7**. Upon dispersion of the oligo(ethylene glycol) (OEG)-derived homopolymer (**3**) in water, poorly defined aggregates were formed (see Fig SI2). In contrast, OEG-grafted polymethacrylate can be molecularly dissolved in water which argues for a role of the poly(norbonene) (**PN**) backbone in contributing to the hydrophobic domains of the aggregates.[29] Surprisingly, for the peptide-based homopolymers **4** and **5**, conventional TEM indicated the formation of vesicular aggregates

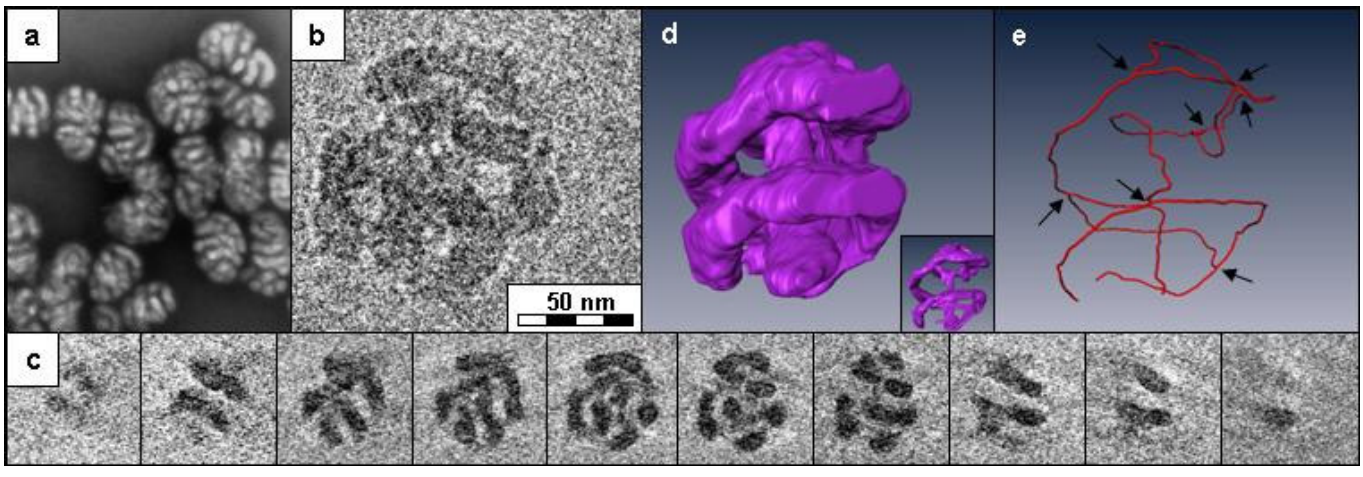

Figure 2. TEM analysis of aggregates of **PNOEG-PNLVL** (**2**)**.** a) Conventional TEM using negative staining, b) cryoTEM image of a vitrified film, c) gallery of z slices showing different cross sections of a 3D volume reconstructed from a tomography series recorded from the vitrified film in b) d) Visualization of the segmented volume before and after (inset) artificial thinning. e) Skeletonization of the aggregate structure high lighting the branching points (arrows)and loops in the aggregate.

(see Fig SI2), despite the fact that they largely consist of water-insoluble material. However, these aggregates had limited stability and rapidly precipitated after which they could not be re-dispersed, suggesting that the hydrophobic **PN-peptide** block is able to undergo conformational rearrangement in aqueous medium. This also implies that the aggregates of **1** and **2** are not simply kinetically trapped states, formed as a consequence of the addition of water, but that the hydrophobic domains are able to adapt their shape and organization such as to minimize the surface energy during the aggregation process.

^{1}H-NMR spectra from the aggregates of **1** and **2** were obtained by freeze-drying the aqueous dispersions and re-dispersing them in D_2O. The only signals visible in the spectra for **1** and **2** were those of the OEG component. (see Fig SI3 and Fig SI4). The absence of any signals representing the poly(norbornene) (**PN**) backbone or peptide side chains suggests that these components are aggregated. ^{1}H NMR relaxation times are influenced by changes in the dynamic motion of protons. T_2 relaxation times decrease as molecular motion decreases and in quasi-glassy cores the signals are broadened beyond detection with NMR.[30, 31] The implication that the hydrophobic regions of the aggregates are formed by not only the peptide side chain but also by the entire **PN** backbone was supported by the finding that also for micellar dispersions of the OEG-derived homopolymer **3** no signals for the **PN** backbone were visible in the ^{1}H-NMR spectra.

The above observations suggest the back folding of the OEG-modified **PN** backbone onto the peptide-modified **PN** part, together forming the hydrophobic domains in the aggregates observed in cryoTEM. This underlines that block copolymers **1** and **2** cannot be considered as simple AB diblock amphiphilic copolymers. It is important to note that the length of the OEG chains (~7 units; extended length of 2.0-2.5 nm) is far less than what is required to fill the hydrophilic domains within the boundaries of the aggregates (approximate dimensions 15 nm for **1** and 20-25 nm for **2**) and that this component will merely form a thin, hydrated layer separating the ~20 nm thick hydrophobic domains from the water.

As both polymers had the same weight fraction of EOG-grafts (W_{OEG} = 0.33, SI2) and comparable molecular weights we attribute the difference in aggregation behavior to the specific amino acid sequence of the peptide graft. In support of this statement we investigated the aggregation behavior of two related polymers **PNOEG-PNGGG** (**6**) and **PNOEG-PNGL** (**7**) which both have the same molecular weight (45kg/mol) and similar W_{OEG} (0.38 for **6** and 0.39 for **7**) but distinctly differ in their aggregation behavior (see SI2). Conventional TEM (Fig. SI2) showed that **PNOEG-PNGGG (6)** formed small clustered micelles of which a number showed a tendency to elongate, whereas **PNOEG-PNGL (7)** surprisingly formed the same spherical aggregates with an internal network structure as were observed for **1** (Fig. 1). The latter observation suggests that the presence of the glycine-leucine sequence, rather than the precise value of W_{OEG} is critical in the formation of the aggregates observed for **1**.

Unfortunately due to strong scattering CD spectroscopy of the aggregate solutions could not provide evidence for higher order structures attributable to the specific organization of the peptides (see Fig SI5).Furthermore FTIR analysis of freeze-dried samples of aggregate solutions of **1** and **2** displayed no compelling evidence for secondary structure formation with amide I bands at 1655cm^{-1} and 1657 cm^{-1} suggesting irregular peptide conformations (see Fig SI6).[32]

The effect of molecular weight, polydispersity and polymer composition on the aggregation of behavior of amphiphilic diblock copolymers has been carefully documented.[6,24, 33] In general a decrease in the weight fraction of the hydrophilic segment(s) leads to a decrease of the spontaneous curvature of the aggregates going from spherical micelles to cylindrical micelles and eventually bilayer aggregates. For polymers with moderate spontaneous curvature it has been demonstrated that also branched structures and highly curved structures can be formed. Although the energy of these aggregates is optimized when these cylinders have a uniform curvature, e.g. in the form of straight rod like structures, system entropy can introduce bending as well as branching of the cylinders. We can consider the aggregates of **1** and **2** as two different types of cylindrical structures with varying degrees of branching.

The branching of cylindrical micelles i.e. both the formation of networks and individual Y-junctions, is associated to defect formation and has been attributed to a frustrated packing of the polymer segments inside the aggregate. Polymer aggregates have been shown not to exchange monomers because of the extremely low CMC of polymer amphiphiles. Consequently, for non-monodisperse polymers such as **1** and **2** (PDI 2.7 and 1.9, respectively, SI2) the aggregates have to accommodate macromolecules with quite different spontaneous curvature. Bates et al have demonstrated that local segregation of polymer chains with the similar length and composition can lead to the formation of regions and segments with different curvature.[33b] We propose that in the present case the polydispersity of **1** and **2** accommodates the formation of branches, folds and loops. More precisely, for **1** the formation of many Y-junctions gives rise to a highly branched, bicontinuous network, where for the aggregates of **2** the surface energy is optimized predominantly by the high curvature of the cylinders, and only to a lower extend by the formation of Y-junctions.

To our knowledge the aggregates observed for **1** and **2** are unique and unprecedented structures. One remarkable aspect of the aggregates of **1** is the fact that the network structure does not extend into solution but seems to be confined within a perforated shell.[34] Similarly, the wormlike structures formed by **2** are extensively folded such that globular architectures are formed (Fig 2a). Although such structures have not yet been observed experimentally until now, both have been described as the results from the molecular modelling of amphiphilic diblock copolymers in which droplets of the polymer were dropped in a water bath after which the phase separation developed inside the confinement of the droplet.[35, 36] Under the experimental conditions used it is conceivable that the dropwise addition of water to a DMSO solution of the polymers causes a phase separation leading to the formation of DMSO-polymer droplets in an aqueous volume. Following from such a situation one may speculate that the subsequent exchange of DMSO against water induces the microphase separation that eventually results in the polymer structures observed.

Importantly, in the above-mentioned simulation of Fraaije and Sevinck the different structures (folded worms, interpenetrating networks) arise as a function of the block length ratios,[35] whereas in the present case these are the result of different peptide sequences in the side chains. However for a given block copolymer system the different structures in the phase diagrams can be also obtained by adjusting the different interaction parameters (χ) which is highly likely to occur upon changing the amino acid sequence in the side chains going from **1** to **2.**

In conclusion we have investigated a new type of double comb diblock copolymer consisting of which one comb polymer blocks contains hydrophilic OEG side chains and the other contains more hydrophobic tripeptide side chains. Upon dispersal in water these form unprecedented aggregates that were analyzed in detail using cryoET. The power of this technique enabled us to establish that the

3D structure of the aggregates was characterized by a high degree of branching and extreme curvature of the essentially micellar assemblies. We demonstrated that the type of aggregates formed was directed by the specific peptide sequence rather than by the hydrophilic-hydrophobic balance of the polymers used, although no evidence was obtained for a specific structural organization of the peptide chains inside the polymer aggregates. One intriguing, and not fully resolved aspect remains that the aggregate structures seem to exist within the apparent spherical boundaries of the droplets that may have formed upon the addition of water to the original polymer-solvent solution. It is reasonable to assume that the relatively broad molecular weight distributions (PDI=1.9-2.7) of the polymers facilitates the formation of such complex morphologies in single aggregate structure by the phase separation into domains with different preferred curvature.

Experimental Section

See supporting information

Received: ((will be filled in by the editorial staff))
Published online on ((will be filled in by the editorial staff))

Keywords: CryoTEM · polymer self-assembly · aggregation · polynorbornene· branching

[1] a) D. E. Discher, A. Eisenberg, *Science* **2002**, *297*, 967-973; b) M. Antonietti, S. Förster *Adv. Mater.* **2003** *15,* 1323-1333.
[2] Z. Li, E. Kesselman,, Y. Talmon, M. A. Hillmyer, T. P Lodge, .*Science* **2004**, *306*, 98-101.
[3] D.J. Pochan, Z. Chen,. H. Cui,. K. Hales, K. Qi, K.L. Wooley, *Science* **2004**, *306*, 94-97.
[4]L. Zhang, C. Bartels, Y. Yu, H. Shen, A. Eisenberg, *Phys Rev. Lett,* **1997**, 79, 5034-5037
[5] J.J.L.M. Cornelissen, M. Fischer, N.A.J.M. Sommerdijk, R. J. M. Nolte, *Science* **1998**, 280, 1427-1430;
[6] S. Jain, F. S. Bates, *Science* **2003**, *300*, 460–464.
[7] a) J. C. M. van Hest, D. A. P. Delnoye, M. W. P. L. Baars, M. H. P. van Genderen, E. W. Meijer, *Science* **1995***, 268*, 1592. b) I. Gitsov, J. M. J.Fréchet, *J. Am. Chem. Soc.* **1996**, *118*, 3785-3786.
[8] a) R. Matmour, R. Francis, R.S. Duran, Y. Gnanou, *Macromolecules* **2005,** *38,* 7754-7767; b) A. Heise, J.L. Hedrick, C.W. Frank, R.D. Miller, *J. Am. Chem. Soc.* **1999**, *121*, 8647-8648.
[9] a) J. Grumelard, A. Taubert, W. Meier, Wolfgang. *Chem. Commun* **2004**, 1462-1463. b) N. Chebotareva, P.H.H. Bomans, P.M. Frederik, N.A.J.M. Sommerdijk, R.P. Sijbesma, *Chem Commun*, 2005, **39**, 4967-4969.
[10] Z. Li, E. Kesselman, Y. Talmon, M.A. Hillmyer, T.P. Lodge, *Science* **2004**, *306*, 98-101. H. Cui, Z. Chen, S. Zhong, K.L. Wooley, D.J. Pochan, Science, **2007,** *317*, 647-650.
[11] S.J. Holder, R.C. Hiorns, N.A.J.M. Sommerdijk, R.G. Jones, R.J.M. Nolte, *Chem Commun* **1998**, 1445; b) N.A.J.M. Sommerdijk, S.J. Holder, R.C. Hiorns, R.G. Jones, R. J.M. Nolte, *Macromolecules* **2000,** *33*, 8289-8294.
[12] E.P. Holowka, V.Z. Sun, D.T.; Kamei, T.J. Deming, *Nat. Mater.* **2007**, *6*, 52-57
[13] a) Y. Geng D.E. Discher J. Justynska H. Schlaad, *Angew. Chem. Int. Ed.* **2006**, *45*, 7578-7581; b) R.M. Broyer, G.M. Quaker, H.D. Maynard,. *J. Am. Chem. Soc.* **2008** *130*, 1041-1047; c) H. Robson Marsden, A.V. Korobko, E.N.M. van Leeuwen, E.M. Pouget, ˙S J. Veen, N.A.J.M. Sommerdijk, A. Kros, *J. Am. Chem. Soc.* **2008** (in press).
[14] a) J.M. Hannink, J.J.L.M. Cornelissen, J.A. Farrera, Ph. Foubert, F.C. De Schryver, N.A.J.M. Sommerdijk, R.J.M. Nolte, *Angew. Chem. Int Ed. Eng.***2001,** *40*, 4732. b) D. Bontempo, H.D. Maynard, *J. Am. Chem. Soc.* **2005**, *127*, 6508-6509.
[15] a) M.J. Boerakker, J.M. Hannink, P.H.H. Bomans, P.M. Frederik, R.J.M. Nolte¸ E. M. Meijer, N.A.J.M. Sommerdijk, *Angew. Chem*., **2002,** 41, 4239. b) K. L. Heredia, D. Bontempo, T. Ly, J. T. Byers, S. Halstenberg, H. D.Maynard, *J. Am. Chem. Soc.* 2005, 127, 16955.
[16] G.W.M. Vandermeulen, K.T. Kim, Z. Wang and I. Manners, Biomacromolecules **2006,** 7, *1005-1010*
[17] H.D. Maynard, S.Y. Okada, R.H. Grubbs, *J. Am. Chem. Soc* **2001**, *123*, 1275-1279.
[18] N.B. Holland, Y. Qiu, M. Ruegsegger, R.E. Marchant, *Nature*, **1998,***392* 799-801.
[19] J.J. Murphy, H. Furusho, R.M.Paton, K. Nomura, *Chem. Eur. J*. **2007**, *13*, 8985 – 8997
[20] L.Tian, P. Nguyen, P.T. Hammond, *Chem. Commun.,* **2006**, 3489–3491.
[21] S.J. Holder, N.A.A. Rossi, C.-T. Yeoh, G.G. Durand, M.J. Boerakker, N.A.J.M Sommerdijk, *J. Mater. Chem* **2003**, *13*, 2771
[22] V Heroguez, Y. Gnanou, M. Fontanille, *Macromolecules,* **1997** *30,* 4791-4798
[23] S.C.G. Biagini, A.L. Parry, *J. Pol. Sci. A* **2007**, *45*, 3178–3190.
[24] N. S.Cameron, M. K.;Corbiere, A.Eisenberg, *Can. J.Chem.* **1999**, *77*, 1311
[25] a) P.M. Frederik, N.A.J.M. Sommerdijk, *Curr. Opn Colloid & Interface Sci.* **2005,** *10*, 245 b) H. Cui, T.K. Hodgdon, E.W. Kaler, L. Abezgauz, D. Danino, M. Lubovsky, Y. Talmon, D.J.Pochan, *Soft Matter* **2007**, **3**, 945-955
[26] a) S. Nickell, C. Kofler, A.P. Leis, W. Baumeister, *Nat. Reviews Mol. Cell Biol.* **2006**, *7*, 225-230, a) P.A. Midgley, Paul E.P.W. Ward, A.B. Hungria, J.M. Thomas, *Chem. Soc. Rev.* **2007**, *36*, 1477-1494
[27] a) M.R.J. Vos, P.H.H. Bomans, F. de Haas, P.M. Frederik, J.A. Jansen, R.J.M. Nolte N.A.J.M. Sommerdijk, *J. Am. Chem. Soc.* **2007***, 129,* 11894; b) T.M. Hermans, M.A.C Broeren, N. Gomopoulos, A.F. Smeijers, B. Mezari, E.N.M. van Leeuwen, M.R.J. Vos, P.C.M.M. Magusin, P.A.J. Hilbers, M.H.P. van Genderen, N.A.J.M. Sommerdijk, G. Fytas, E. W. Meijer, *J. Am. Chem. Soc.* **2007***, 129*, 15631.
[28] Due to the practical limitation of the tilt-series to angles between -70^{o} and +70^{o} the so-called "missing wedge" effect (see also ref 26) causes artifacts in the reconstruction, in the form of an parent stretching of the features which is most pronounced in the z direction. As the aggregates appear isotropic, i.e. randomly oriented and without any preferred (structural) orientation, the measurements were made in the XY projections of the z-slices.
[29] a) S. Han, M. Hagiwara, T. Ishizone , Macromolecules **2003**, 36, 8312-8319. (b) JF Lutz, A Hoth, Macromolecules **2006**, 39, 893-896.
[30] a) J. Godward, F. Heatley, C. Price, *J. Chem. Soc. Faraday Trans.*, **1993**, 89, 3471-3475; b) Franco Cau and Serge Lacelle *Macromolecules* **1996,** *29,* 170-178; c) J. Kříž , B. Masař, H. Pospížil, J. Pleštil, Z. Tuzar, and M. A. Kiselev *Macromolecules* **1996,** *29,* 7853-7858
[31] The presence of both cis and trans double bonds (ratio 15/85) may be of some importance to the folding properties of the **PN** back bone, however no further evidence to support this suggestion is available at the moment.
[32] H. Fabian, C.P. Schultz, *"Fourier Transform Infrared Spectroscopy in Peptide and Protein Analysis"* in *Encyclopedia of Analytical Chemistry,* Ed.: Meyers, R.A., John Wiley & Sons Ltd., Chichester, pp. 5779-5803.
J. Kubelk,a T.A. Keiderling, *J. Am. Chem. Soc.* **2001,** *123,* 12048-12058
[33] a) S.A. Safran, *Surface Science* **2002**, *500* 127–146; b) S. Jain, F.S. Bates, *Macromolecules* **2004**, *37,* 1511-1523.
[34] Objects with similar appearance (in projection) have been observed by Eisenberg and coworkers upon addition of NaCl to vesicles of polystyrene-polyacrylic acid block copolymers, however detailed TEM investigations of these structures under diffent tilt angles revealed that these intermediates were dissimilar to the structures observed in the present study: K. Yu, C. Bartels, A. Eisenberg, *Langmuir* **1999,** *15,* 7157-7167.
[35] J. G. E. M. Fraaije and G. J. A. Sevink *Macromolecules,* 2003 *36,* 7891
[36] Fraaie and Sevink (ref 35) also predicted the formation of globules of closely associated of spherical micelles. These aggregates strongly resemble the clusters of miceles observed for PNOEG-PNGGG. However, due to the absence of detailed 3 dimensional morphological data we can not further confirm the structural resemblance between the two structures.

Entry for the Table of Contents

complex block copolymer morphologies

Alison L. Parry, Paul H.H. Bomans, Simon J. Holder*, Nico A.J.M. Sommerdijk* and Stefano C.G. Biagini*_____ **Page – Page**

Cryo-Electron Tomography reveals Confined Complex Morphologies from Tripeptide-containing Amphiphilic Double Comb Diblock Copolymers

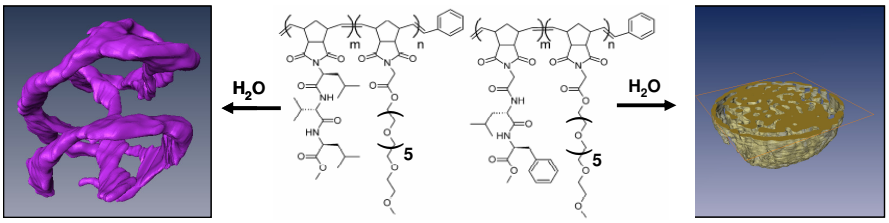

Amphiphilic norbornene-based double comb diblock polymers with peptide and oligo(ethylene oxide) side chains aggregate in water to form unprecedented complex morphologies depending on the amino acid sequence of the peptide. Cryo-electron tomography reveals the internal structure of the aggregates showing densely folded and highly branched worm-like micelles (left) and spherical aggregates with a bicontinuous internal structure (right).

Supporting information

SI1. Experimental Section

Materials and Equipment

Preparation of polymer dispersions

A sample of block copolymer (10 mg) was dissolved in filtered DMSO (3cm^3). Filtered water (7cm^3) was added drop-wise to the vigorously stirred polymer solution at a flow rate of 5.6 cm^3/hour. Samples were transferred and dialysed against distilled water (pH 6.9) using dialysis membranes (Medicell International Ltd, Size 5, Inf Dia 24/32" - 19.0mm) with a cut off of approximately 12000-14000 Daltons. The dialysis was performed during 48 hours to obtain a final concentration of copolymer in water of 1 g/dm^3. The water (1 dm^3) surrounding the dialysis bag was changed three times during this procedure. Water (HPLC grade, Fisher) and DMSO (99.9% HPLC Grade, Fisher) were filtered using Sartorious Minisart 0.20µm filters.

^{1}H NMR spectroscopy

270 MHz ^{1}H spectra were recorded on a JEOL GX-270 FT spectrometer at ambient temperature. Spectra were referenced internally to the residual protons in the NMR solvent.

FTIR spectroscopy

FT-IR spectra for freeze-dried samples from aggregate solutions of **1** and **2** were recorded on a Nicolet 380 FT-IR instrument using the Smart-Orbit ATR accessory with a diamond crystal (32 scans, 4 cm^{-1} resolution).

CD spectroscopy

CD spectra were recorded on a JASCO J-600 spectropolarimeter using a scan rate of 10 nm per min, a bandwidth of 1 nm and a response time of 1 s. Four accumulations were collected for each sample. The concentration of the aqueous polymer dispersions was 1 gL^{-1}.

GPC

Molecular weight determinations were performed by Rapra Technology using a Waters 150C instrument with two PLgel MIXED-C columns in series with a refractive index detector. DMSO was used as the eluent. Molecular weights were estimated relative to Pharmacia dextran 'T' fraction broad distribution calibrants. Lithium bromide was added to the DMSO which was eluted at a flow rate of 1.0 ml/min at 80 °C.

Dynamic Light Scattering (DLS)

Dynamic light scattering measurements were performed on a Malvern High Performance Particle Sizer (HPPS HPP5001) with a wavelength λ=633nm. The temperature was fixed at 25 °C and samples were allowed to equilibrate to this temperature before measurements were recorded. Three runs with an average of 14 scans each were performed. Data was analysed with HPPS Malvern Dispersion Technology Software version 3.00.

Conventional Transmission Electron Microscopy (cTEM)

TEM was carried out using a JEOL JEM-1230 operating at 80 kV. Samples were deposited onto copper EM grids prior to analysis. One drop of the prepared aggregate solution was placed onto a 200 mesh formvar coated copper EM grid, blotted with filter paper and stained with a solution of uranyl acetate (1% w/v in water).

Cryogenic Transmission Electron Microscopy (cryoTEM)

CryoTEM was performed in low dose mode using a Gatan cryo-holder operating at ~ -170 °C and an FEI Titan Krios TEM equipped with a field emission gun (FEG) operating at 300 kV. Images were recorded using a 2k x 2k Gatan CCD camera equipped with a post column Gatan energy filter (GIF). The sample vitrification procedure was carried out using an automated vitrification robot, viz. a FEI Vitrobot™ Mark III. The Quantifoil grids were made hydrophilic with a surface plasma treatment using a Cressington 208 carbon coater operating at 5 mA for 40 seconds prior to the sample preparation and vitrification.

Cryogenic ElectronTomography (cET)

For cET a sample was prepared containing streptavidin-gold (6 nm) which was purchased from Aurion. A tilt series of 141 images from -70° to + 70° was recorded using the FEI explore 3D software (settings:tilt increment: 1^{o}; I/I_{60} =1.6; Δfocus = -2 μm). The tomography reconstruction was performed using the Inspect 3D software package using manual bead tracking and employing the SIRT projection algorithm. Additional image processing was performed using Amira version 4.1.

SI2. Polymer characteristics

Polymer	nr	Th M_n [a]	Th. DP [a]	Mn $GPC_{(DMSO)}$ [b]	DP $GPC_{(DMSO)}$ [b]	W_{OEG} [c]
PNOEG-PNGLF	**1**	52936	100	52100	98	0.33
PNOEG-PNLVL	**2**	52533	100	37800	72	0.33
PNOEG	**3**	27754	50	27500	49	-
PNGLF	**4**	24856	50	18800	38	-
PNLVL	**5**	25259	50	7170	14	-
PNOEG-PNGGG	**6**	45923	100	55000	120	0.38
PNOEG-PNGL	**7**	45174	100	39800	88	0.39

[a] Determined from $[M]_0/[C]_0$=50/1 and based on the observed 100% conversion (see manuscript ref 23) ; [b] Calculated from GPC with DMSO as the eluant; [c] Weight fraction of OEG in block copolymer.

SI3. Dynamic Light Sattering

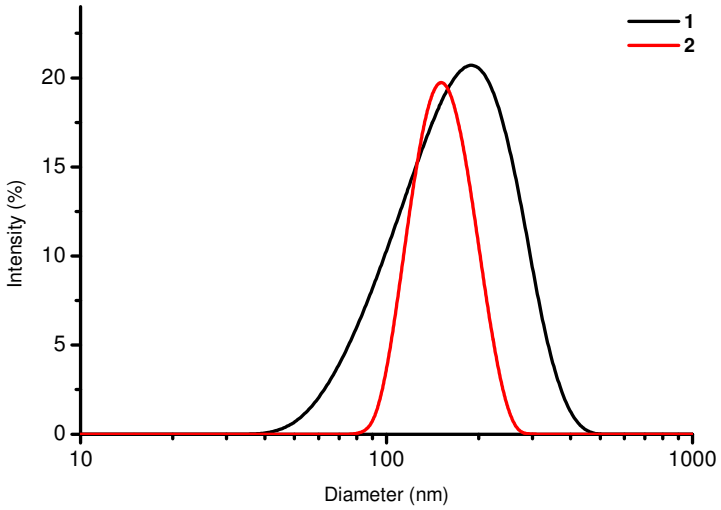

Figure SI1. DLS particle size distribution of the aggregates of **1** and **2** in aqueous dispersion.

SI4 Conventional TEM imaging

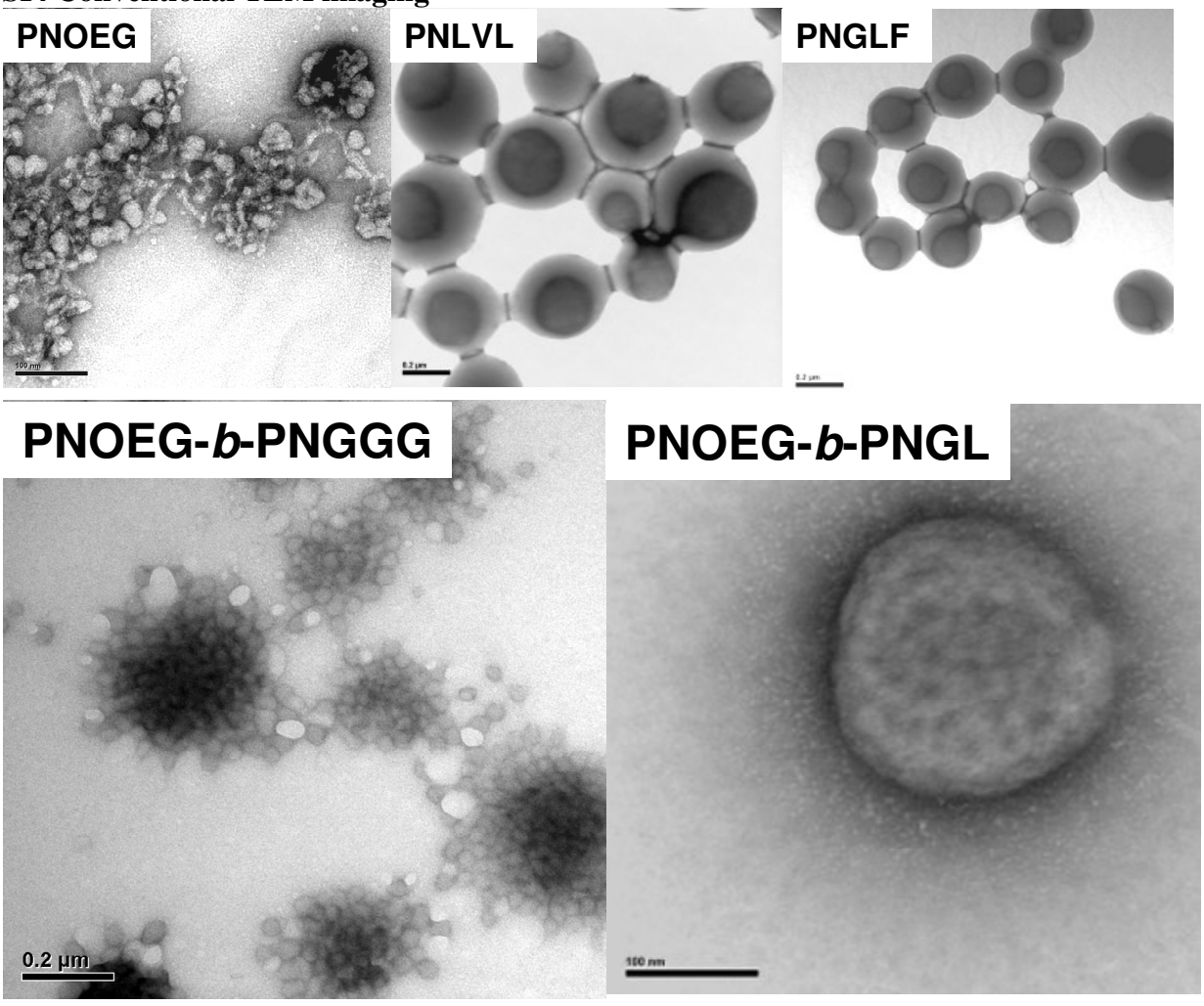

Figure SI2. cTEM images of the aggregates of polymers 3-7 (negative staining)

SI5. ^{1}H NMR spectroscopy

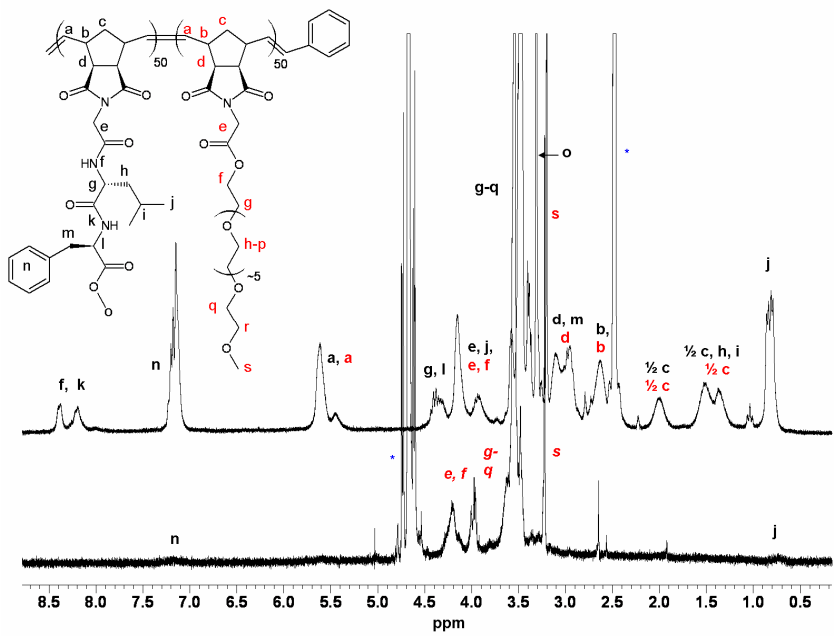

Figure SI3. ^{1}H NMR spectra of **1** in $CDCl_3$ (upper trace) and D_2O (lower trace)

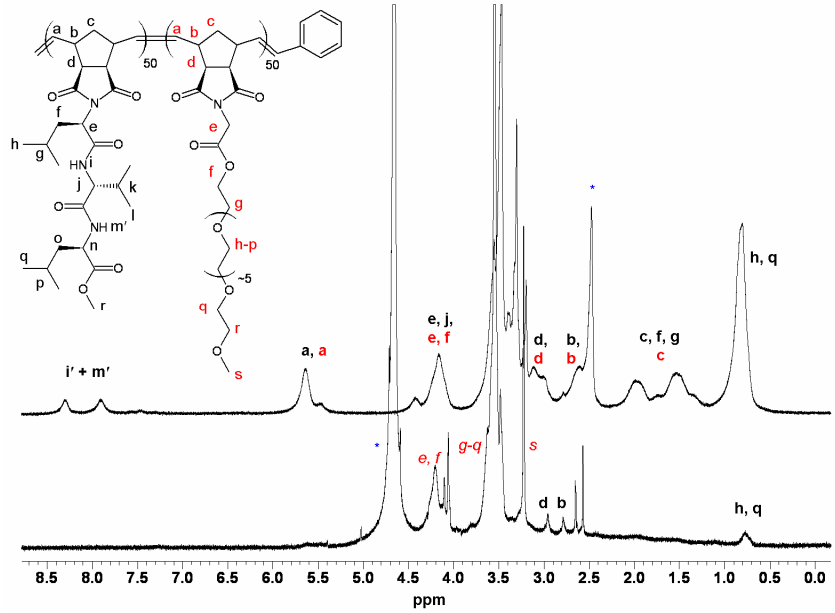

Figure SI4. ^{1}H NMR spectra of **2**in $CDCl_3$ (upper trace) and D_2O (lower trace)

SI6. Circular dichroism

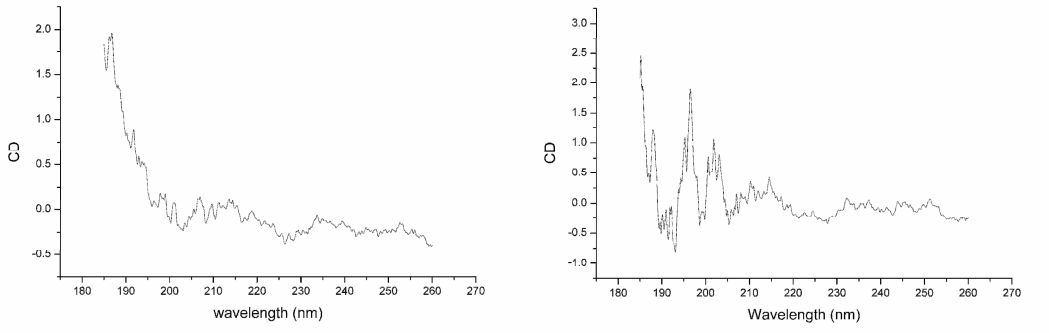

Figure SI5. Uncorrected CD spectra of aqueous dipersions of **1** (left) and **2** (right)

SI7. FTIR spectra

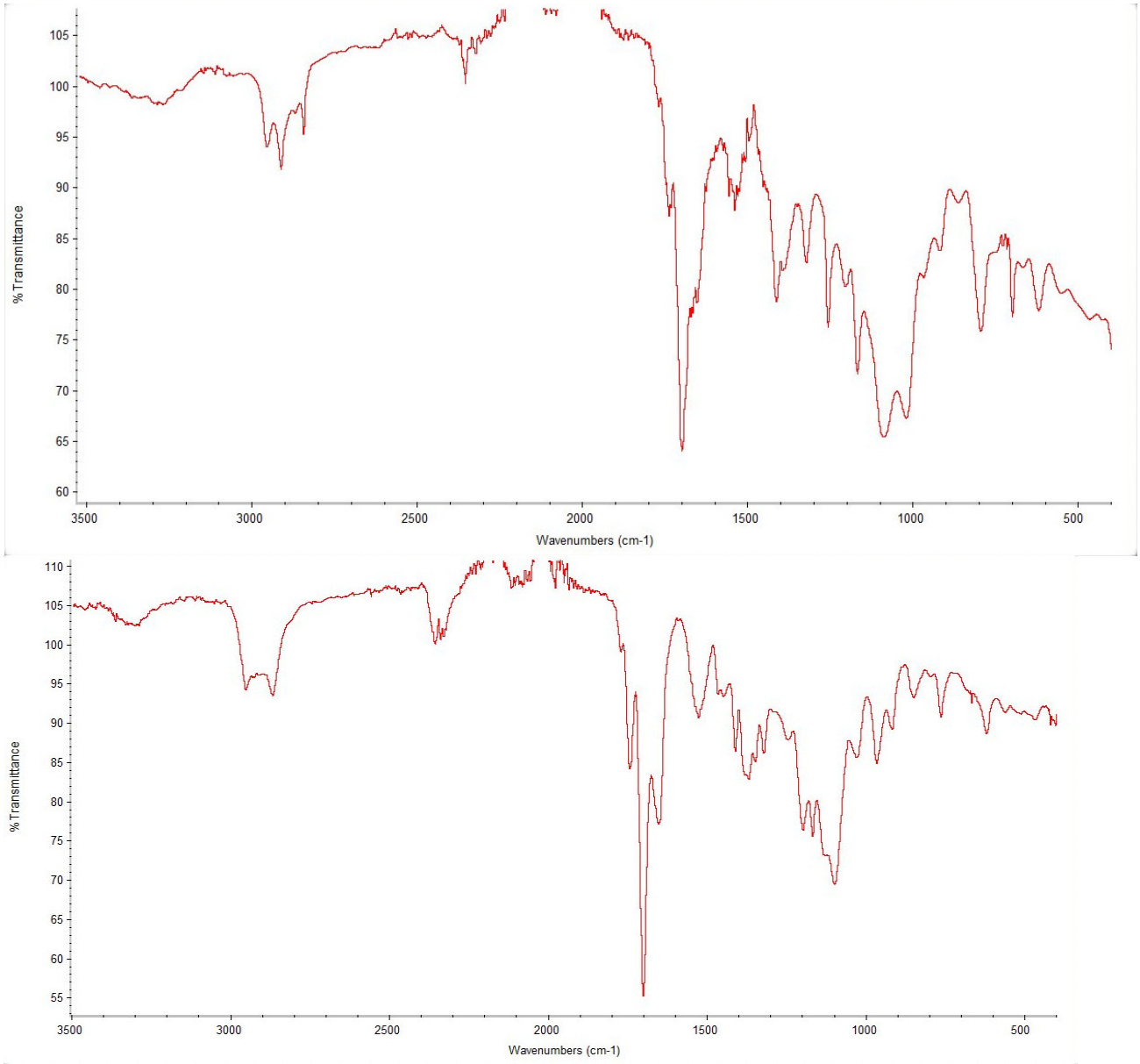

Fig SI6. FTIR spectra of freeze dried suspesions of **1** (top) and **2** (bottom) .

.